

# A mononuclear, and terminal titanium(III) imido

Jacob S. Mohar,<sup>a</sup> Anders Reinholdt,<sup>a</sup> Taylor M. Keller,<sup>a</sup> Patrick J. Carroll,<sup>a</sup> Joshua Telser,<sup>b,\*</sup> and Daniel J. Mindiola<sup>a,\*</sup>

We report the first mononuclear  $Ti^{III}$  complex possessing a terminal imido ligand. Complex  $[Tp^{tBu,Me}Ti\{≡NSi(CH_3)_3\}(THF)]$  (2) ( $Tp^{tBu,Me}$  = hydridotris(3-tert-butyl-5-methylpyrazol-1-yl)borate) is prepared by reduction of  $[Tp^{tBu,Me}Ti\{≡NSi(CH_3)_3\}(Cl)]$  (1) with  $KC_8$  in high yield. The connectivity and metalloradical nature of 2 were confirmed by single crystal X-ray diffraction studies (scXRD), Q- and X-band EPR as well as UV-Vis and  $^1H$  NMR spectroscopies. The  $d^1$  complex  $[(Tp^{tBu,Me}TiCl(OEt_2)][B(C_6F_5)_4]$  (3), was prepared in order to spectroscopically compare it to 2. Electrochemical studies of 1 and 2 reveal a reversible  $1e^-$  process, whereas chemical oxidants  $ClCPH_3$  or  $\frac{1}{2}$  eq.  $XeF_2$  cleanly yield 1 or the fluoride derivative  $[Tp^{tBu,Me}Ti\{≡NSi(CH_3)_3\}(F)]$  (4), respectively, with the latter being fully characterized including a scXRD study.

Early transition metal (group III-VI) imidos ( $RN^{2-}$ ) have been studied extensively for the past 60 years due to their utility in stoichiometric<sup>1</sup> and catalytic reactions.<sup>2</sup> Specifically, titanium imidos have shown great utility in Ziegler-Natta polymerization,<sup>2b,3</sup> cycloaddition,<sup>4</sup> group transfer,<sup>1b,5</sup> hydroamination,<sup>5b,6</sup> C-H bond activation,<sup>7</sup> carboamination,<sup>8</sup> and hydrogenation reactions.<sup>7b,9</sup> The earliest reports of  $Ti^{IV}$  imidos, by Bradley *et al.*, date back to 1963 followed by the first structural characterization of a polymeric  $Ti^{IV}$  imido complex containing bridging imido and chloride ligands,  $[Ti\{μ-NSi(CH_3)_3\}(μ-Cl)Cl]_n$ , reported by Alcock *et al.* in 1974.<sup>10</sup> Not until 1990 when Hill *et al.* reported a terminal, mononuclear  $Ti^{IV}$  imido did two distinct classes of Ti imidos displaying either bridging or terminal coordination emerge.<sup>9b,11</sup> Both coordination modes of Ti imidos are dominated by diamagnetic,  $Ti^{IV}$  centers with mononuclear and terminal  $Ti^{III}$  imidos entirely eluding isolation, in spite of being isoelectronic with the ubiquitous vanadyl ion,  $\{V≡O\}^{2+}$ , a system which helped establish the present-day understanding of metal-ligand

multiple bonds.<sup>9b,12</sup> Dinuclear  $Ti^{III}$  imido systems, however, have been reported in both coordination modes. Cummins *et al.* showed the reduction of complex  $[(^tBu_3SiNH)(THF)(R)Ti\{≡NSi^tBu_3\}]$  ( $R = Me, ^tBu$ ) with  $H_2$  yielded  $[(^tBu_3SiNH)Ti\{μ-NSi^tBu_3\}]_2$ , **Fig 1A**, representing the first example of  $Ti_2^{III,III}$  bridging imidos.<sup>7b</sup> Later, Bai *et al.* reported the ligand fragmentation product  $K_2\{η^2-ArNC(CH_3)CHC(CH_3)\}(ArN)Ti(μ-H)\}_2$  ( $Ar = 2,6-iPr_2C_6H_3$ , **Fig 1B**), representing a  $Ti_2^{III,III}$  complex containing terminal imidos.<sup>13</sup> Other examples include the mixed valence  $Ti_2^{III,IV}$  complex  $[CoCp_2][(C_5R_5)Ti(Cl)\{μ-NAr\}]_2$  ( $R = H, Me; Ar = 3,5-(CF_3)_2C_6H_3$ ) by Tsurugi *et al.* containing two bridging imidos (**Fig 1C**),<sup>14</sup> and, more recently, the  $Ti_2^{III,III}$  complex  $[K(18-crown-6)(THF)_2][(NIm^{Ar})(NAd)Ti(μ-NAd)_2Ti(NIm^{Ar})(K)]$  ( $NIm^{Ar} = 1,3$ -bis( $Ar$ )imidazolin-2-iminato;  $Ar = 2,6-iPr_2C_6H_3$ ;  $Ad = adamantly$ ) containing one terminal and two bridging imidos by Gómez-Torres, *et al* (**Fig 1D**).<sup>15</sup> Inspired by these advances, and given our recent success in isolating a pseudo-tetrahedral  $Ti^{II}$  center,<sup>16</sup> we sought to expand the chemistry of Ti imidos by synthesizing and fully characterizing a mononuclear and terminal  $Ti^{III}$  imido as described herein.

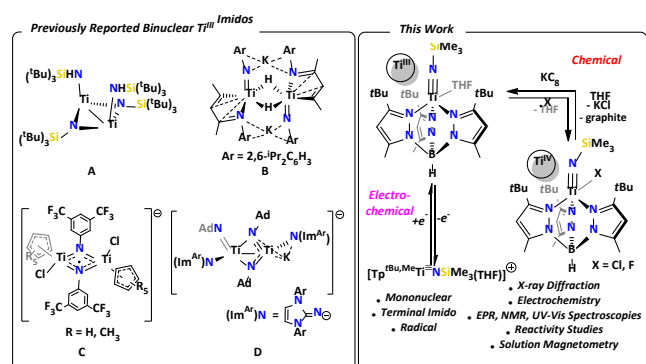


**Fig 1.** Left: Previous examples of isolated and structurally characterized dinuclear  $Ti^{III}$  imido complexes A-D. Cations for C ( $CoCp_2^+$ ), and D ( $K(18-crown-6)(THF)_2^+$ ) are omitted for clarity. Right: This work: a mononuclear, terminal  $Ti^{III}$  imido displaying redox reactivity.

<sup>a</sup> Department of Chemistry, University of Pennsylvania, 231 S 34<sup>th</sup> Street  
Philadelphia, Pennsylvania, United States

\*Corresponding Authors: mindiola@sas.upenn.edu; jtelsler@roosevelt.edu

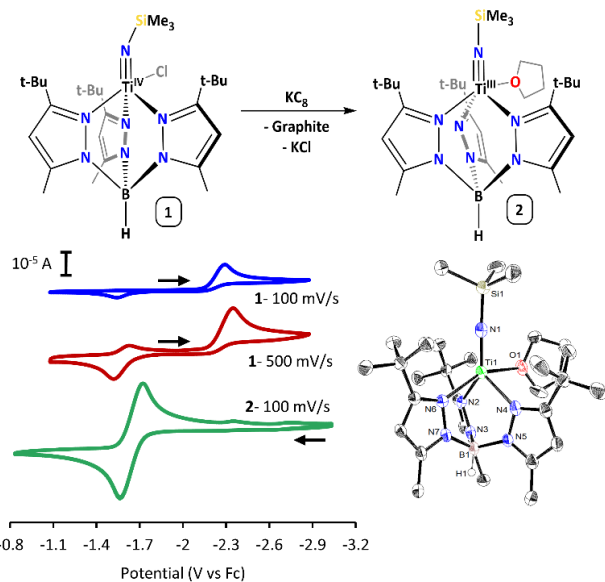


**Fig 2.** Top: Reduction of **1** to **2**. Bottom Left: CV of **1** (3.0 mM **1**, 0.215 M [ $^n\text{Bu}_4\text{N}$ ] $[\text{PF}_6]$ ) in THF) collected at various scan rates and **2** (3.4 mM **2**, 0.271 M [ $^n\text{Bu}_4\text{N}$ ] $[\text{PF}_6]$ ) in THF) collected at a scan rate of 100 mV/s. All referenced to  $\text{Fc}^{+/0}$  couple at 0.0 V. Bottom Right: Thermal ellipsoid plot of **2** (50% probability level) with hydrogen atoms (except for H1) and residual  $\text{Et}_2\text{O}$  omitted for clarity.

Previously, our group reported the  $\text{Ti}^{\text{IV}}$  imido complex  $[(\text{Tp}^{\text{tBu},\text{Me}})\text{Ti}\{\equiv\text{NSi}(\text{CH}_3)_3\}(\text{Cl})]$  (**1**) ( $\text{Tp}^{\text{tBu},\text{Me}}$  = hydridotris(3-*tert*-butyl-5-methylpyrazol-1-yl)borate) formed upon deazotation of  $(\text{CH}_3)_3\text{SiN}_3$  by  $[(\text{Tp}^{\text{tBu},\text{Me}})\text{TiCl}]$ .<sup>16</sup> Cyclic voltammetry studies (CV) of **1** at slow scan rates (50 and 100 mV/s) revealed an irreversible reduction event at -2.32 V as well as an irreversible oxidation event at -1.53 V vs  $\text{Fc}^{+/0}$ , **Fig 2** (blue trace). The latter oxidation feature becomes quasi-reversible at faster scan rates ( $\geq 150$  mV/s,  $E_{1/2\text{red}} = -1.61$  V,  $E_{1/2\text{ox}} = -1.53$  V, **Fig 2**, red trace). These quasi-reversible features are dependent on the reduction event at -2.32 V and thus not observed in CV scans sweeping potentials  $>-1.9$  V (see SI for details). We initially assigned the reduction event at -2.32 V to a  $[(\text{Tp}^{\text{tBu},\text{Me}})\text{Ti}\{\equiv\text{NSi}(\text{CH}_3)_3\}(\text{Cl})]^{0/-}$  redox couple, for which a subsequent chloride dissociation step leads to electrochemical irreversibility and the quasi-reversible features at -1.61/-1.53 V to a  $[(\text{Tp}^{\text{tBu},\text{Me}})\text{Ti}\{\equiv\text{NSi}(\text{CH}_3)_3\}(\text{THF})]^{+/0}$  redox couple. To probe this, 1-4 eq. [ $^n\text{Bu}_4\text{N}$ ] $[\text{Cl}]$  were added to the electrolyte solution causing the quasi-reversible reduction event (-1.61 V) to disappear. This suggests a hypothetical cationic species such as  $[(\text{Tp}^{\text{tBu},\text{Me}})\text{Ti}\{\equiv\text{NSi}(\text{CH}_3)_3\}(\text{THF})]^{+}$  to rapidly associate with  $\text{Cl}^-$  to form complex **1** with high concentrations of  $\text{Cl}^-$  and with  $\text{PF}_6^-$  under low concentrations of chloride (See SI and discussion below for details). It also suggests that the  $\text{PF}_6^-$  coordinated  $[(\text{Tp}^{\text{tBu},\text{Me}})\text{Ti}\{\equiv\text{NSi}(\text{CH}_3)_3\}(\text{THF})]^{+}$  is easier to reduce than **1** (*vide infra*). In any case, the reduction event at -2.32 V suggested the possibility of chemical reduction of **1** to a  $\text{Ti}^{\text{III}}$  species, which under electrochemical conditions seemed unstable.

Accordingly, chemical reduction of **1** with one equivalent of  $\text{KC}_8$  in THF yielded a yellow-brown microcrystalline material in 91% yield after work-up, identified as  $[(\text{Tp}^{\text{tBu},\text{Me}})\text{Ti}\{\equiv\text{NSi}(\text{CH}_3)_3\}(\text{THF})]$  (**2**), **Fig 2**, on the basis of structural and spectroscopic studies (*vide infra*). Room temperature  $^1\text{H}$ -

NMR spectroscopy revealed significantly broadened and paramagnetic shifts for the pyrazolyl, B-H, and trimethylsilyl resonances (ESI, Fig S3.1.1). Solution state magnetometry determined *via* Evans method<sup>17</sup> (300 K in benzene- $d_6$ ) revealed  $\mu_{\text{eff}} = 1.85 \mu_{\text{B}}$  consistent with a spin-only  $d^1$  system.

Single crystal X-ray diffraction studies (scXRD) of **2**, **Fig 2**, revealed an unprecedented, terminally-bound, and mononuclear  $\text{Ti}^{\text{III}}$  imido with a short  $\text{Ti}\equiv\text{NR}$  length of 1.766(6) Å. The  $\text{Ti}\equiv\text{NR}$  bond length is only  $\sim 0.06$  Å longer than the same metrical parameter found in the  $\text{Ti}^{\text{IV}}$  precursor **1**, 1.692(1)-1.700(2) Å,<sup>16,18</sup> in line with the larger ionic radius of  $\text{Ti}^{\text{III}}$  versus the  $\text{Ti}^{\text{IV}}$  ion (0.67 vs 0.42 Å, respectively).<sup>19</sup> The  $\text{Ti}\equiv\text{NR}$  bond distance in **2** is in good agreement with the  $\text{Ti}\equiv\text{NR}$  bond distance of 1.770(4) Å in the  $\text{Ti}_{2}^{\text{III},\text{III}}$  terminal imido and the difference from its  $\text{Ti}^{\text{IV}}$  analogue ( $\sim 0.04$  Å) reported by Bai *et al.*, **Fig 1B**.<sup>13</sup> The  $\text{Ti}\equiv\text{NR}$  bond length in complex **2** is however, longer than the terminal  $\text{Ti}\equiv\text{NR}$  bond distance of 1.729(3) Å reported recently by Gomez-Torres *et. al.*<sup>15</sup> Additionally, the  $\angle\text{Ti}\equiv\text{N}-\text{Si}$  in **2** was found to be 172.6(4)°, which is more obtuse than the same angles of 158.94(10)-160.24(9)° found in precursor **1**.<sup>16,18</sup> We attribute the near-linear topology of the  $\{\text{Ti}\equiv\text{N}-\text{Si}\}$  core in **2** to the increase in the size of and change of geometry (**1**:  $\tau_5 = 0.47-0.59$ , **2**:  $\tau_5 = 0.29$ ) about the Ti-center which lies an average of 0.17 Å further from the tris-pyrazole (NNN) plane (see SI for details)<sup>16,18</sup> and enables the imido ligand to minimize steric repulsion with the bulky  $\text{Tp}^{\text{tBu},\text{Me}}$  ligand and become almost perfectly linear in **2**.

To better understand why **1** gave rise to two separate redox events and to determine if indeed the  $\text{Cl}^-$  was interfering with reversibility, we collected CV data for **2**. We found that **2** possesses a fully reversible redox event at  $E_{1/2} = -1.64$  V vs  $\text{Fc}^{0/+}$ , which we attribute to the  $\text{Ti}^{\text{III}}/\text{Ti}^{\text{IV}}$  redox couple, **Fig 2** (green trace in Figs 2 and S7.2.2). No significant features were observed around -2.3 V (Fig S7.2.3). The reversible feature at -1.64 V for **2** coincides with the irreversible oxidation/reduction peaks observed at -1.53/-1.61 V for **1** (*vide supra*), which suggests that one-electron oxidation of **2** to form a hypothetical  $[\mathbf{2}^+][\text{PF}_6^-]$  salt becomes reversible when chloride ions are absent and a background of  $[\text{PF}_6^-]$  is present and suggests that  $[(\text{Tp}^{\text{tBu},\text{Me}})\text{Ti}\{\equiv\text{NSi}(\text{CH}_3)_3\}(\text{THF})]^{+}$  is more easily reduced than **1** (see SI for details). This feature also suggests that one-electron oxidation of **2** at the electrode surface to form hypothetical  $[\mathbf{2}^+][\text{PF}_6^-]$  involves minimal reorganization energy due to the weakly coordinating nature of  $\text{PF}_6^-$  unlike with  $\text{Cl}^-$  (*vide supra*).

To better understand the electronic structure of **2**, we prepared a close structural and electronic analogue  $[(\text{Tp}^{\text{tBu},\text{Me}})\text{TiCl}(\text{OEt}_2)][\text{B}(\text{C}_6\text{F}_5)_4]$  (**3**<sup>Et<sub>2</sub>O</sup>) independently from oxidation of  $[(\text{Tp}^{\text{tBu},\text{Me}})\text{TiCl}]^{16}$  with  $[\text{Ti}][\text{B}(\text{C}_6\text{F}_5)_4]$  in  $\text{Et}_2\text{O}$  in 65.7% yield (ESI, Section 2.3). The THF complex,  $[(\text{Tp}^{\text{tBu},\text{Me}})\text{TiCl}(\text{THF})][\text{B}(\text{C}_6\text{F}_5)_4]$ , (**3**<sup>THF</sup>), was analogously prepared but proved more challenging to purify. These cationic chloride complexes were chosen as close structural analogues of **2** to assess the perturbation of the electronic structure of the  $d^1$  ion caused by the multiple bond character of the imido group and to assess the role of a dative ligand such as THF. Akin to **2**, the solution magnetic susceptibility measurement of **3**<sup>Et<sub>2</sub>O</sup> yielded

$\mu_{\text{eff}} = 1.86 \mu_{\text{B}}$  at 300 K in THF- $d_8$  in good agreement with a spin-only  $d^1$  species. To further probe the electronic structure of **2**, we turned to UV-vis spectroscopy, **Fig 3**. The  $d^0$  precursor, **1**, unsurprisingly, displays no absorption bands in the range 500–750 nm (THF or toluene solvent). In contrast, **2** and **3** (**3<sup>THF</sup>**) each display a low-intensity feature consistent with a  $d-d$  transition: **2**: 618 nm ( $\epsilon = 225 \text{ cm}^{-1} \cdot \text{M}^{-1}$ ) in toluene and 659 nm ( $\epsilon = 110 \text{ cm}^{-1} \cdot \text{M}^{-1}$ ) in THF (pink and green traces in **Fig 3** respectively); **3** (**3<sup>THF</sup>**): 574 nm ( $\epsilon = 30 \text{ cm}^{-1} \cdot \text{M}^{-1}$ ) in THF and (**3<sup>Et<sub>2</sub>O</sup>**): 584 nm ( $\epsilon = 56 \text{ cm}^{-1} \cdot \text{M}^{-1}$ ) in  $\text{Et}_2\text{O}$  (black and blue trace in **Fig 3** respectively).

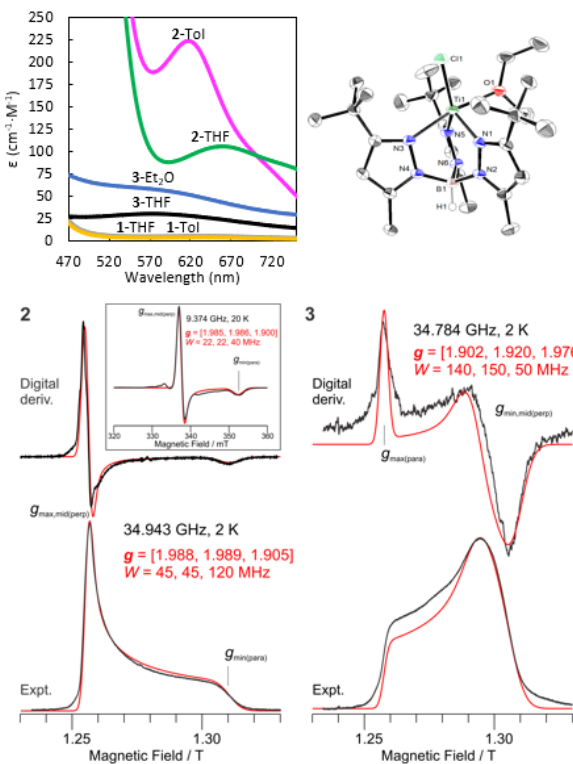


**Fig 3:** Top left: UV-vis spectrum of **1**, **2**, and **3** in solvents listed (Tol = toluene). Top right: X-ray structure of **3<sup>Et<sub>2</sub>O</sup>** (50% probability level) with H atoms (except for H1), residual  $\text{Et}_2\text{O}$ , and  $[\text{B}(\text{C}_6\text{F}_5)_4]^-$  omitted for clarity. Bottom Left: EPR spectra of **2** in Tol/THF frozen solution (black traces; simulations as red traces with  $S = 1/2$  parameters as shown). Main figure: Q-band (34.943 GHz, 2 K) spectrum. Experimental spectrum is in absorption mode due to rapid passage effects and is shown with a digital derivative above for comparison with conventional (first derivative) EPR. Inset: X-band (9.374 GHz, 20 K) spectrum in first derivative (slow passage) mode. Features not reproduced in the simulations are due to  $^{47,49}\text{Ti}$  hyperfine coupling (See SI for details). Bottom right: EPR spectrum of **3<sup>Et<sub>2</sub>O</sup>** in Tol frozen solution.

The solvent-dependence in the intensity and absorption energy for electronic transitions in complex **2** are consistent with dissociation of the THF ligand in toluene to form a putative four-coordinate  $\text{Ti}^{IV}$  imido  $[(\text{Tp}^{\text{tBu},\text{Me}})\text{Ti}\{\equiv\text{NSi}(\text{CH}_3)_3\}]$ . In a previous study, it was found that an isoelectronic  $\text{V}^{IV}$  nitrido complex,  $[(\text{Tp}^{\text{tBu},\text{Me}})\text{V}\equiv\text{N}\}(\text{THF})]$ , readily expels THF in weakly coordinating solvents.<sup>20</sup> The near order of magnitude increase in molar absorptivity between **3** and **2** reflects the forbidden nature of  $d-d$  transitions occurring in **3** (selection rule for orbital quantum number:  $\Delta l = \pm 1$ ), versus the more allowed  $d_{xy} \rightarrow \pi^*_{\text{Ti}\equiv\text{N}}$  transitions in **2** (excitations to molecular orbitals with titanium

and nitrogen parentage), which is consistent with the bonding and spectroscopic properties for a  $d^1$  systems having metal-ligand multiple bonds developed by Ballhausen and Gray for the isoelectronic vanadyl ion,  $\{\text{V}\equiv\text{O}\}^{2+}$ .<sup>12</sup>

Further spectroscopic evidence for the presence of a Ti-centric radical in **2** was obtained through continuous wave (CW) X- and Q-band EPR spectroscopy. Surprisingly, **2** exhibited an axial  $S = 1/2$  spectrum ( $g_{x(\text{max})} \approx g_{y(\text{mid})} \approx g_{\perp} > g_{z(\text{min})} = g_{\parallel}$ ) in toluene and toluene/THF glasses, **Fig 3**, (X-band,  $g_{x,y,z} = [1.985, 1.986, 1.900; g_{\text{avg}} = 1.957]$ , 20 K; Q-band,  $g_{x,y,z} = [1.988, 1.989, 1.905]$ , 2 K) despite its low symmetry observed in the solid state by scXRD. This axial EPR, as would be expected for a trigonally symmetric four-coordinate complex, is however consistent with the results of UV-Vis spectroscopy (*vide supra*). The  $g$  values observed for **2** display a pattern similar to  $\{\text{V}\equiv\text{O}\}^{2+}$ , in which  $g_{\perp}$  is closer to  $g_e$  (2.00) than  $g_{\parallel}$  due to the energetic ordering of the V 3d orbitals in triply-bonded  $\{\text{V}\equiv\text{O}\}^{2+}$ , and in line with the electronic structure of **2** being strongly defined by  $\{\text{Ti}\equiv\text{NSiMe}_3\}$  bonding.<sup>12,24</sup> In contrast to UV-vis spectral studies (*vide supra*), there is no change in the  $g$ -values when CW-X-band EPR was collected using 1:1 THF:toluene glass or toluene glass. Hence, the periphery of the  $\{\text{Ti}\equiv\text{NR}\}^+$  fragment have minimal effect on the magnetic properties of **2**. No hyperfine coupling to the imido nitrogen was detected by EPR indicating that the unpaired electron is metal centered and in a  $d_{xy}$  orbital orthogonal to the  $\text{Ti}\equiv\text{NR}$  bond. In comparison, the EPR spectrum of **3<sup>Et<sub>2</sub>O</sup>** is also roughly axial, but with ( $g_{x(\text{min})} \approx g_{y(\text{mid})} \approx g_{\perp} < g_{z(\text{max})} = g_{\parallel}$ ; Q-band,  $g_{x,y,z} = [1.902, 1.920, 1.976]$ , 2 K) and is thus similar, albeit less rhombic, to the neutral, five-coordinate complex  $[\text{Tp}^{\text{tBu},\text{Me}}\text{Ti}^{IV}\text{Cl}_2]$  reported previously.<sup>16</sup> We propose the EPR differences between **2** and **3** to result from the stronger  $\pi$ -donation of the imido compared to the chloride.<sup>21</sup> Further comparisons among EPR spectra of **3** as a function of temperature and solvent are given in the SI.

Taking advantage of the radical nature of **2**, we chemically probed its electrochemical features (*vide supra*); oxidation of **2** with  $\text{ClCPH}_3$  quantitatively formed **1** along with Gomberg's dimer as evidenced by  $^1\text{H-NMR}$  spectroscopy (Fig S3.2.1).<sup>22</sup> In an attempt to desilylate **2** with 0.5 equivalents of  $\text{XeF}_2$ , we instead observed the formation of the imido-fluoride  $[(\text{Tp}^{\text{tBu},\text{Me}})\text{Ti}\{\equiv\text{NSi}(\text{CH}_3)_3\}(\text{F})]$ , **4**, in 86% yield, **Fig 4**. Complex **4** is resistant to  $\text{FSiMe}_3$  elimination even under forcing conditions (70 °C, 18 hrs) and metrically, the structures of **1** and **4** are quite similar with a short  $\text{Ti}\equiv\text{NSiMe}_3$  bond distance and slightly bent  $\angle\text{Ti}\equiv\text{N}-\text{Si}$  (Table in **Fig 4**). The geometries at Ti are also quite similar when judged by their  $\tau_5$  values (Table in **Fig 4**). The room temperature  $^{19}\text{F-NMR}$  spectrum of **4** exhibits one sharp resonance at +131.4 ppm, and unlike **1**, complex **4** undergoes rapid Berry pseudo-rotation on the NMR time scale (300 K) resulting in equivalent pyrazolyl moieties in solution (ESI, Fig S3.4.1).<sup>23</sup> Unsurprisingly and akin to **1**, complex **4** displays no absorption bands in the 500–750 nm range (Fig S5.4.1).

We have provided conclusive evidence for the synthesis of the first mononuclear,  $\text{Ti}^{IV}$  complex containing a terminal imido ligand,  $\{\text{Ti}\equiv\text{NR}\}^+$ . Electrochemical and chemical reversibility of the interconversion between  $\text{Ti}^{IV}$  imido **1** and  $\text{Ti}^{III}$  imido **2** were probed electrochemically (CV) and chemically *via* reduction

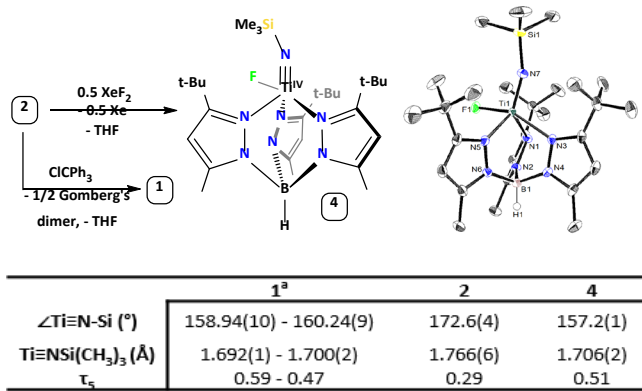


**Figure 4:** Top left: Reactivity of **2** with  $\text{ClCPPh}_3$  and  $\text{XeF}_2$  to form **1** and **4** respectively. Bottom Top right: Thermal ellipsoid plot of **4** (50% probability level) with hydrogen atoms (except for H1) and residual  $\text{Et}_2\text{O}$  omitted for clarity. Bottom: Table of the structural parameters of compounds **1**, **2**, and **4**. <sup>a</sup>Previously reported.<sup>16</sup>

(oxidation) with potassium graphite (trityl chloride). We observed no evidence for desilylation of the imido upon treatment of the  $\text{Ti}^{III}$  center with an electrophilic fluoride source ( $\text{XeF}_2$ ) and instead form a  $\{\text{Ti}-\text{F}\}$  bond, **4**. In probing the radical nature of **2**, we provided evidence from EPR of  $\{\text{Ti} \equiv \text{NSiMe}_3\}$  bonding of a Ti-centered radical having axial symmetry, where the unpaired electron resides in a d-orbital perpendicular to the orbitals involved in  $\pi$ -donation from the imido ligand  $\{\text{V} \equiv \text{NR}\}^{2+}$  and resembling the well-known vanadyl unit,  $\{\text{V}=\text{O}\}^{2+}$ .

## Conflicts of interest

There are no conflicts to declare.

## Acknowledgements

The authors wish to acknowledge Amy Metlay and Dr. Rolando Aguilar for helpful discussions surrounding the structure and electrochemistry of **2**. D.J.M. thanks the U.S. NSF; Grants CHE-0848248 and CHE-1152123) and the University of Pennsylvania. J.T. also thanks the NSF (Grant MCB-1908587). We thank Prof. Brian M. Hoffman (Northwestern University, Evanston, IL) for use of EPR spectrometers, supported by the NIH (grant GM-111097).

## Notes and references

- (a) P. J. Walsh, F. J. Hollander and R. G. Bergman, *J. Am. Chem. Soc.*, **1988**, *110*, 8729-8731. (b) E. W. Harlan and R. H. Holm, *J. Am. Chem. Soc.*, **1990**, *112*, 186-193. (c) P. Legzdins, E. C. Phillips, S. J. Rettig, J. Trotter, J. E. Veltheer and V. C. Yee, *Organometallics*, **1992**, *11*, 3104-3110. (d) V. C. Gibson, C. Redshaw, W. Clegg and M. R. J. Elsegood, *J. Chem. Soc., Chem. Commun.*, **1994**, 2635. (e) D. L. Morrison and D. E. Wigley, *Inorg. Chem.*, **1995**, *34*, 2610-2616. (f) J. I. Fostvedt et al., *Chem. Sci.*, **2020**, *11*, 11613-11632.
- (a) W. A. Nugent and B. L. Haymore, *Coord. Chem. Rev.*, **1980**, *31*, 123-175. (b) S. M. Rocklage, R. R. Schrock, M. R. Churchill and H. J. Wasserman, *Organometallics*, **1982**, *1*, 1332-1338. (c) T. R. Cundari, *J. Am. Chem. Soc.*, **1992**, *114*, 7879-7888. (d) R. R. Schrock and A. H.

Hoveyda, *Angew. Chem., Int. Ed.*, **2003**, *42*, 4592-4633. (e) K. Kawakita, B. F. Parker, Y. Kakiuchi, H. Tsurugi, K. Mashima, J. Arnold and I. A. Tonks, *Coord. Chem. Rev.*, **2020**, *407*, 213118.

- (a) G. Tejeda, D. S. Belov, D. A. Fenoll, K. L. Rue, C. Tsay, X. Solans-Monfort and K. V. Bukhryakov, *Organometallics*, **2022**, *41*, 361-365. (b) Y. Jin, Y. Yang, C. Su, J. Wang, Y. Wang and B. Liu, *Macromol. React. Eng.*, **2022**, *16*, 2200025. (c) N. A. H. Male, et al., *Inorg. Chem.*, **2000**, *39*, 5483-5491. (d) N. Adams et al., *Chem. Commun.*, **2004**, 434-435. (e) J. Jin, W. R. Mariott and E. Y. X. Chen, *J. Polym. Sci., Part A: Polym. Chem.*, **2003**, *41*, 3132-3142.
- (a) S. M. Pugh, et al., *Organometallics*, **2000**, *19*, 3205-3210. (b) A. E. Guiducci, C. L. Boyd and P. Mountford, *Organometallics*, **2006**, *25*, 1167-1187. (c) A. J. Blake, J. M. McInnes, P. Mountford, G. I. Nikonov, D. Swallow and D. J. Watkin, *J. Chem. Soc., Dalton Trans.*, **1999**, 379-392.
- (a) S. P. Heins, P. T. Wolczanski, T. R. Cundari and S. N. Macmillan, *Chem. Sci.*, **2017**, *8*, 3410-3418. (b) P. L. McGrane and T. Livinghouse, *J. Am. Chem. Soc.*, **1993**, *115*, 11485-11489. (c) T. E. Hanna, I. Keresztes, E. Lobkovsky, W. H. Bernskoetter and P. J. Chirik, *Organometallics*, **2004**, *23*, 3448-3458.
- Y. Li, Y. Shi and A. L. Odom, *J. Am. Chem. Soc.*, **2004**, *126*, 1794-1803.
- (a) M. Fischer, M. Manßen, M. Schmidtmann, T. Klüner and R. Beckhaus, *Chem. Sci.*, **2021**, *12*, 13711-13718. (b) C. C. Cummins, C. P. Schaller, G. D. Van Duyne, P. T. Wolczanski, A. W. E. Chan and R. Hoffmann, *J. Am. Chem. Soc.*, **1991**, *113*, 2985-2994.
- (a) Z. W. Davis-Gilbert, L. J. Yao and I. A. Tonks, *J. Am. Chem. Soc.*, **2016**, *138*, 14570-14573. (b) Z. W. Gilbert, R. J. Hue and I. A. Tonks, *Nat. Chem.*, **2016**, *8*, 63-68.
- (a) B. M. Hoffman, D. Lukyanov, Z.-Y. Yang, D. R. Dean and L. C. Seefeldt, *Chem. Rev.*, **2014**, *114*, 4041-4062. (b) C. Lorber, *Coord. Chem. Rev.*, **2016**, *308*, 76-96. (c) N. Hazari and P. Mountford, *Acc. Chem. Res.*, **2005**, *38*, 839-849.
- (a) D. C. Bradley and E. G. Torrible, *Can. J. Chem.*, **1963**, *41*, 134-138. (b) N. W. Alcock, M. Pierce-Butler and G. R. Willey, *J. Chem. Soc., Chem. Commun.*, **1974**, 627a-627a.
- J. E. Hill, R. D. Profleet, P. E. Fanwick and I. P. Rothwell, *Angew. Chem., Int. Ed.*, **1990**, *29*, 664-665.
- C. J. Ballhausen and H. B. Gray, *Inorg. Chem.*, **1962**, *1*, 111-122.
- G. Bai, P. Wei and D. W. Stephan, *Organometallics*, **2006**, *25*, 2649-2655.
- H. Tsurugi, H. Nagae and K. Mashima, *Chem. Commun.*, **2011**, *47*, 5620-5622.
- A. Gómez-Torres, N. Mavragani, A. Metta-Magaña, M. Murugesu and S. Fortier, *Inorg. Chem.*, **2022**, *61*, 16856-16873.
- A. Reinholdt et al., *Inorg. Chem.*, **2020**, *59*, 17834-17850.
- (a) D. F. Evans, *J. Chem. Soc.*, **1959**, 2003-2005. (b) S. K. Sur, *J. Mag. Res. (1969)*, **1989**, *82*, 169-173. (c) G. A. Bain and J. F. Berry, *J. Chem. Ed.*, **2008**, *85*, 532.
- A range for the Ti-imido bond distances in **1** is presented as three inequivalent molecules of **1** make up the unit cell of **1** as previously reported.
- R. D. Shannon, *Acta Cryst. A*, **1976**, *32*, 751-767.
- M. G. Jafari, et al., *J. Am. Chem. Soc.*, **2022**, *144*, 10201-10219.
- V. C. Gibson, *J. Chem. Soc., Dalton Trans.*, **1994**, 1607-1618.
- M. Gomberg, *J. Am. Chem. Soc.*, **1900**, *22*, 757-771.
- (a) C. Serre, T. Corbière, C. Lorentz, F. Taulelle and G. Férey, *Chem. Mater.*, **2002**, *14*, 4939-4947. (b) R. S. Berry, *J. Chem. Phys.*, **1960**, *32*, 933-938.
- D. Baute, D. Goldfarb, *J. Phys. Chem. A*, **2005**, *109*, 7865-7871

TOC Graphic

